Automotive and Engine Technology (2024) 9:7
https://doi.org/10.1007/s41104-024-00145-3

ORIGINAL PAPER

Influence of the air–fuel-ratio and fuel on the reactivity of diesel soot

Christian Böhmeke[1] · Uwe Wagner[1] · Thomas Koch[1]

Received: 17 July 2024 / Accepted: 4 September 2024

Abstract
This work deals with the influence of the variation of the air–fuel-ratio on the emissions as well as on the soot reactivity of a commercial vehicle diesel engine. The emissions and the associated soot reactivity are compared between conventional fossil diesel fuel and the regeneratively produced paraffinic diesel fuel HVO (hydrotreated vegetable oils). All investigations were carried out on a single-cylinder engine and the gaseous and particulate emissions were recorded. Additionally, the collected engine out soot samples were analyzed by thermogravimetric balance (thermogravimetric analysis = TGA) to determine the reactivity of the soot. Regardless of the set engine operating point, it was shown that the particulate mass is significantly reduced when operating with HVO compared to fossil diesel fuel. Other gaseous emissions are also minimally lower compared to fossil diesel. In contrast, however, the HVO fuel has an increased number of particles due to smaller particles. The variation of the engine operating parameters showed the same tendencies with regard to soot reactivity, regardless of the fuel used. However, the parameter variations were more or less pronounced depending on the respective fuel. It is particularly noticeable that the reactivity of soot, which is produced when using HVO, is reduced at every operating point despite the lower particulate mass compared to fossil diesel fuel.

Keywords Emissions · Soot reactivity · HVO · Diesel engine

Abbreviations

AFR	Air fuel ratio
bTDC	Before top dead center
CA	Crank angle
CO	Carbon monoxide
CO_2	Carbon dioxide
DPF	Diesel particulate filter
EGR	Exhaust gas recirculation
FAME	Fatty acid methyl ester
FSN	Filter smoke number
GfG	Graphite spark generator soot
HVO	Hydrotreated vegetable oils
HRR	Heat release rate
IMEP	Indicated mean effective pressure
Lambda λ	Air–fuel equivalence ratio
MFB	Mass fraction burned
NO_x	Nitrogen oxides
O_{20}	Oxygen
Phi ϕ	Fuel–air equivalence ratio
PM	Particulate mass
PN	Particulate number
RI	Soot reactivity index
SOE	Start of energizing
TGA	Thermogravimetric analysis
THC	Total hydrocarbons
VOC	Volatile organic compounds

1 Introduction

Due to the heterogeneous combustion in diesel engines, particulate formation can be hardly avoided completely. Resulting particulate emissions are regulated by law both in terms of their mass and the number of particles emitted. To comply with these limits, diesel particulate filters (DPF) are used as standard in passenger cars and commercial vehicles. As a result of the particles emitted, a layer of soot builds up in the DPF, which increases the exhaust back pressure of the engine and reduces efficiency, thereby increasing fuel consumption [1]. For this reason, the soot stored in the DPF must be oxidized regularly. This regeneration is largely determined by the reactivity of the soot and thus by

✉ Christian Böhmeke
christian.boehmeke@kit.edu

[1] Institute of Internal Combustion Engines (IFKM), Karlsruhe Institute of Technology (KIT), Rintheimer Querallee 2, Karlsruhe 76131, Deutschland

Published online: 12 September 2024

its physicochemical properties. More reactive soot therefore ensures time- and consumption-efficient regeneration [2]. However, the loading in the particle filter has the advantage of increased filtration efficiency, as it is much more difficult for the particles to penetrate when the particle filter is filled [3]. In addition to the engine operating parameters, different fuels also exhibit differences in terms of the reactivity of the soot [4].

1.1 State of the art

In the past, several studies were published on the influence of various engine parameters on soot reactivity. Lindner [5] showed that by increasing the air–fuel-ratio, soot reactivity was increased by increasing only the air mass and leaving the other parameters unchanged. The reason given here is the reduction in soot formation and the increase in soot oxidation due to increased cylinder pressures. This in turn leads to more amorphous soot structures, which generally have a positive effect on soot reactivity, as less energy is required to oxidize the soot with oxygen on the soot surface [6, 7]. Su et al. [8] investigated two different engines with regard to their soot reactivity. The significant differences in soot reactivity were attributed to different primary particle sizes. Increased soot reactivity was found with smaller particle diameters. This in turn was attributed to improved mixture preparation and a higher air–fuel-ratio, resulting in a larger specific surface area. Chughtai et al. [9] found the same results with model flame soot, where larger specific surface areas with increased air–fuel-ratios lead to increasing soot reactivity. This contrasts with the investigations by Mehring et al. [10], in which soot samples with a low air–fuel-ratio exhibited the highest reactivities. The reason given for this is the incomplete combustion, which should result in the formation of looser soot structures, which in turn allow better penetration of the oxygen molecules during oxidation.

In addition to the influence of engine operating parameters, influences of the fuel properties on soot reactivity have also been investigated in the past. Song et al. [11] showed the higher reactivity of biodiesel (B100) compared to a Fischer–Tropsch diesel. A 6-cylinder turbocharged HD-engine was used as the test vehicle at a speed of 2400 rpm and 25% load. The reason given here is the inclusion of greater oxygen functionality on the surface of the B100 soot, which exhibits faster oxidation and a modified soot structure. Lapuerta et al. [12] also investigated the influence of biodiesel on the increased reactivity. Here, the smaller particle diameter of biodiesel soot was given as a reason and thus also the changed soot structure. This nanostructure is dependent on the fuel and the combustion conditions and determines the physical and chemical properties of the soot [13]. Amorphous regions consist of polycyclic aromatic compounds such as graphene precursors in a disordered and onion-like orientation, whereas graphitic regions are more ordered and oxidation is more difficult here [14]. Jansma et al. [15] investigated the soot properties of several fuels. It was particularly noticeable that fuels with a high aromatic content (especially diaromatics) lead to a significantly increased soot reactivity compared to fuels with little or no aromatics. This is due to a crystalline and ordered structure and therefore fewer defects in their structure, which means that more energy is required for oxidation.

2 Experimental setup and methodology

The test rig setup and the analytical methods used to characterize the various influences on soot reactivity are described below.

2.1 Engine and test bench specifications

All tests were carried out on a 2.0 l MTU BR2000 single-cylinder research engine with common rail injection system. The technical data are shown in Table 1.

The schematic test bench setup is shown in Fig. 1. Thermodynamic evaluation of the engine was done by cylinder, intake and exhaust manifold pressure indication using Kistler type 6061B and 4075A pressure transducers. The conditioning of oil, cooling water, intake air and fuel was controlled externally. The engine was operated at constant oil and water temperature of 90 °C and an intake air temperature of 40 °C. A freely programmable engine control unit (FI2RE) allowed the injection to be set variably. To determine the externally controlled exhaust gas recirculation rate (EGR), the CO_2 emissions were measured before and after the engine (ABB URAS AO2000).

2.2 Investigated engine operating parameters and fuels

As described at the beginning, soot oxidation reactivity depends on various engine operating parameters and the fuel used. For this reason, this study deals with the influence of the AFR-equivalence ratio λ ($\lambda = 1/\phi$) and the

Table 1 Engine specifications

MTU BR2000	
Displacement	1.99 dm^3
Bore	130 mm
Stroke	150 mm
Compression ratio	13.3: 1
Number of valves	4
Injector	Bosch CRIN3-25

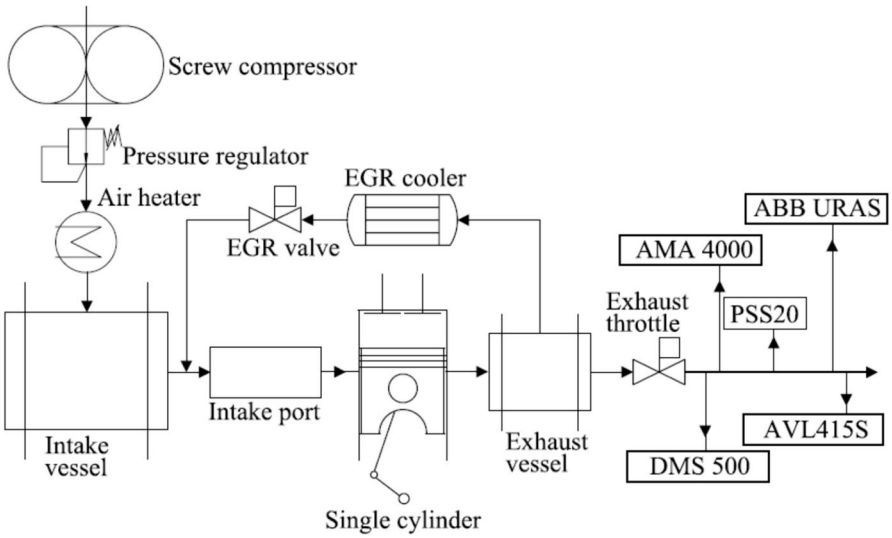

Fig. 1 Schematic test bench

Table 2 Investigated engine operating parameters

Engine Speed / rpm	IMEP / bar	Rail pressure / bar	EGR / %	SOE/ °CA bTDC	λ / –
1300	11.1	1200	25	21.9 / 11.9	1.4
1300	11.4	1200	25	21.9 / 11.9	1.6
1300	11.5	1200	25	21.9 / 11.9	1.8

Table 3 Fuel properties

Description	Unit	Diesel B0	HVO
Density (15 °C)	kg / m3	831.4	781.3
Lower heating value	MJ / kg	42.84	43.6
Cetane number	–	57.5	65.3
Carbon mass fraction	%	86.0	85.1
Hydrogen mass fraction	%	13.97	14.9
Oxygen mass fraction	%	0.01	0.01
Total aromatics	%	26.5	< 0.5
Polyaromatic HC	%	2.6	< 0.2
H/C ratio	–	1.936	2.086
Flash point	°C	64.5	85
Stoichiometric air–fuel ratio	–	14.61	14.94

difference in fuel formulation. A typical part-load base operating point of a diesel engine, which was derived from the base application of the series production full-cylinder engine (MTU BR2000) at the respective speed and load, serves as a reference. Table 2 provides an overview of the parameters set. To vary the air–fuel-ratio, the boost pressure and thus the air mass was changed. The injection pressure (rail pressure), the start of energizing (SOE), the EGR-rate and the injected fuel mass were kept constant. Furthermore, a pilot injection was set 10 degrees before the main injection for each operating point. By increasing the boost pressure and the resulting higher air mass and earlier center of combustion (Mass fraction burned = MFB_{50}), the indicated mean effective pressure (IMEP) increases moderately [16].

To investigate the influence of different fuel formulations in addition to the engine parameters, a fossil diesel fuel B0 according to DIN EN590 without fatty acid methyl ether (FAME) content and a purely paraffinic diesel substitute fuel, which is referred to as HVO, were used. The fuel properties are shown in Table 3. As the HVO fuel is almost free of aromatics, it has a significantly higher cetane number compared to fossil diesel [17, 18]. It should also be noted that HVO has a higher gravimetric calorific value. Nevertheless, HVO has a lower density, so that despite its higher calorific value, the volumetric calorific value is lower, which means that less energy can be carried in the fuel tank in real operation [19].

2.3 Measurement of gaseous, particulate emissions and soot samples

Different measuring systems were used to evaluate the emissions of the various operating parameters and fuels. An exhaust gas measuring system (AMA 4000 AVL) was used to determine the gaseous emissions (THC, CO, CO_2, NO_x, O_2). In addition, a Fourier transform infrared spectrometer (FTIR IAG) was used for non-regulated gaseous exhaust gas components (e.g. NH_3, formaldehyde, isocyanic acid) and to validate the nitrogen oxide emissions of the exhaust gas measuring system. In the test series, the components were measured according to the manufacturer's “diesel recipe” stored in the device. This was used independently of the fuel. Particulate emissions were analyzed in terms of mass and number. A smokemeter (SM 419 AVL), which detects

the Filter Smoke Number (FSN), was used to determine the mass, while a particle spectrometer without volatile particle remover (DMS500 Cambustion) was used to determine the number of particles (PN) and the corresponding size distribution. This enables the measurement of particles in a size range from 4.8 to 1000 nm. A dilution of 180 (first dilution level = 6 / second dilution level = 30) was set for all operating points. When calculating the particle size distributions, the measurements were each averaged over 90 s.

In addition to the emissions examined during operation, soot samples were also collected in the exhaust gas and analyzed ex-situ. A partial flow dilution system (Particulate Sampling System PSS 20) with a dilution of 3:1 was used to collect soot samples on quartz fiber filters (type QR-100, 47 mm). A thermogravimetric analysis (TGA) was used to determine the soot reactivity of the soot samples. This decisive analysis technique is described in the following chapter.

2.4 Soot oxidation reactivity / thermogravimetric analysis

The oxidation reactivity of soot, also known as soot reactivity, is one of the most important variables to describe the oxidation behavior of the emitted engine soot. This physicochemical property has a significant influence on particulate filter regeneration process with regard to temperature, efficiency and duration [20]. The soot reactivity is a measure of the reaction rate of oxidation and thus describes the reactivity [21, 22]. An established method is the thermogravimetric analysis [21], which was also used in this work. The temperature at which the maximum oxidation rate of soot occurs is referred to as T_{Max} and is used as an indicator of reactivity [23]. An oxidative conversion of soot only starts at temperatures above around 350 °C. Below these temperatures, in the so-called low temperature range, volatile organic compounds (VOC) may evaporate. A high T_{Max} value corresponds with low reactivity, and therefore a higher oxidation temperature is required. A soot reactivity index (RI) can be introduced with the help of two known oxidation reactivities (1). Graphite spark generator soot (GfG soot) with a maximum reactivity at 500 °C and graphite with a maximum reactivity at 770 °C are used here [24].

$$RI_{SOOT} = \left[\frac{T_{Sample} - T_{Graphite}}{T_{GfG} - T_{Graphite}}\right] \quad (1)$$

The measuring principle of thermogravimetric analysis is based on the continuous decrease in mass of the soot sample during oxidation as a function of temperature and/or time [20]. As a result of the analysis with subsequent derivation according to temperature, a temperature-dependent oxidation profile is obtained (see Fig. 2). This profile is also referred to as a Gram-Schmidt diagram. To

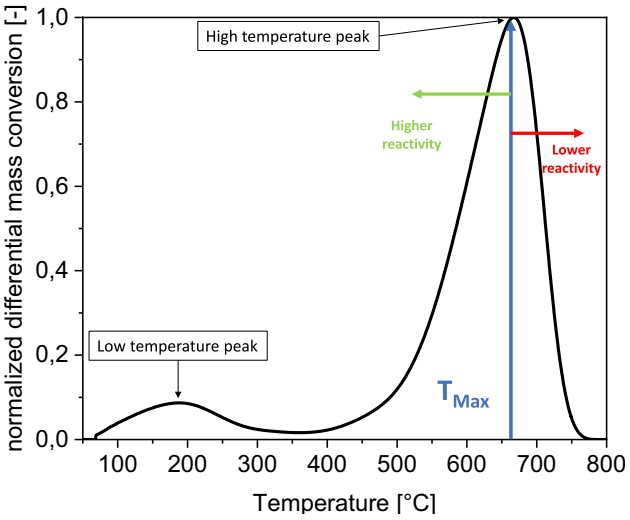

Fig. 2 Example mass conversion rate (TGA profile)

investigate the oxidation rates of the different soot samples, a thermobalance (TG 209 F1 Libra Netsch Gerätebau GmbH) was operated with a synthetic gas flow of 5 vol-% O_2 and 95 vol-% N_2. The constant heating rate was set to 5 K/min in a temperature range from 50 to 750 °C.

The conditions for error calculation of the AMA 4000 analyzers, determined by noise, linearity, zero drift, and reproducibility, are specified in the "Technical Data" section by the manufacturer. The analysis was conducted considering the worst-case scenario. The same approach is used for the fuel consumption and air mass flow rate. The uncertainty of the in-cylinder pressure measurement chain, based on crank angle, is explicitly stated in the manufacturer's manual as well as the filter smoke number. The uncertainty in particle size distribution measurement remains a highly complex issue and is currently under ongoing discussion. Consequently, manufacturers report varying maximum deviations for different particle diameters. The measurement accuracy of the thermobalance is also shown. Only the uncertainty for the measuring device is shown here; the influence of the sample collection and the engine is not considered. The extended uncertainties derived from these calculations are presented in Table 4.

3 Results and discussion

In the following, the results of the variation of the air–fuel-ratio and the different fuels are compared with regard to thermodynamics, emissions and soot reactivity. Furthermore, the soot reactivity based on the thermodynamic influences and especially the particle emissions were correlated.

Table 4 Uncertainties of measured parameters and ranges

Measured parameter	Analyzer	Analyzer range	Max uncertainty
HC emission	AMA FID 4000 HHD	0–20,000 [ppm]	2 [% of measured value]
NO_x emission	AMA CLD 4000 HHD	0–10,000 [ppm]	1 [% of measured value]
O_2 emission	AMA PMD 4000	0–25 [%]	0.5 [% of measured value]
CO emission	AMA IRD 4000	0–5000 [ppm]	1 [% of measured value]
CO_2 emission	AMA IRD 4000	0–20 [%]	1 [% of measured value]
Particle number	Cambustion DMS 500 Fast aerosol sizer	5–1000 [nm] $0–10^{11}$ [dN/dlogD_p/cc]	10 nm: 1.0×10^3 [dN/dlogD_p/cc] 30 nm: 4.0×10^2 [dN/dlogD_p/cc] 100 nm: 1.7×10^2 [dN/dlogD_p/cc] 300 nm: 8.0×10^1 [dN/dlogD_p/cc]
FSN	AVL Smokemeter 415S	0–10 [-]	0,005 [FSN + 3% of measured value]
Air mass flow rate	Aerzener Rotary gas meter Zc 11.3	2.5–400 [m3/h]	1 [% of measured value]
Fuel consumption	AVL KMA 4000 Typ 150	0–110 [kg/h]	0.1 [% of measured value]
In-cylinder pressure trace	DEWETRON 800 / Kistler 6061B sensor	0–250 [bar]	2 [% of measured value]
Soot reactivity T_{Max}	Netsch TG 209 F1 Libra	50–1200 [°C]	0.2 [°C]

3.1 Thermodynamic analysis

One of the most important combustion process variables in diesel engine combustion with regard to soot formation and soot oxidation processes within the engine is the air–fuel-ratio. As described in chapter 2.2, the air mass was increased or reduced to vary the air–fuel-ratio. All other operating parameters such as EGR-rate, SOE and rail pressure were kept constant. Figure 3 shows the comparison of the cylinder pressure traces and the gas temperatures calculated from the ideal gas equation. The gas mass from compressed air, fuel and EGR rate was determined for this purpose. Furthermore, the heat release rate was calculated from the pressure curve using engine process calculation. Higher boost pressures go along with higher in-cylinder mass and higher in-cylinder pressure for increased air–fuel-ratio. This contrasts with the lower gas temperatures at higher air–fuel-ratios due to the higher proportion of inert gas. Both fuels exhibit the same behavior here. In addition, a slightly lower gas temperature, especially for an air–fuel-ratio of $\lambda = 1.4$ and $\lambda = 1.6$, can also be observed when operating with HVO. This can be attributed to the longer energization time of the injector and thus the greater volume of fuel introduced, as the volumetric calorific value of HVO is lower than that of fossil diesel B0. The injected fuel mass hardly differs, as approximately the same fuel mass was injected due to the small differences in the gravimetric calorific value. With regard to the heat release rates (HRR), it can be seen HVO combustion starts earlier compared to B0 diesel due to the higher cetane number of HVO and thus the shorter ignition delay time. This is significantly more pronounced for the ignition and combustion of the pre-injection, but still visible for the main injection. It should also be noted that due to the lower cetane number in diesel and lower peak pressure at an air–fuel-ratio of $\lambda = 1.4$, the proportion of premixed combustion is higher.

3.2 Gaseous and particulate emissions

Figure 4 shows the influence of the air–fuel-ratio on the gaseous emissions and the particulate mass. As the combustion air–fuel-ratio increases, a sharp decrease in particulate mass can be seen due to the higher oxygen concentration. On the other hand, there is a strong increase in nitrogen oxide (NO_x) emissions. This soot-NO_x trade-off is typical for diesel engines. Carbon monoxide (CO) emissions also fall significantly with a higher air–fuel-ratio due to the less rich areas. Although total hydrocarbon (THC) emissions increase slightly, they remain constant at a low level. In general, it can be stated that all emissions show the same trends regardless of the fuel used, but the particulate mass of HVO is significantly lower than the particulate mass of diesel. The gaseous emissions with HVO are moderately below those with diesel.

Figure 5 shows the different particle size distributions and the total number of particles in the tests. As the air–fuel-ratio decreases, the number of particles increases, as does the particle mass. This trend can be seen for both fuels. However, an increased particle number emission can be seen when using HVO, which is higher than the particle number emission of diesel. This becomes clear from the particle size distribution, although HVO causes more particles, they are also significantly smaller, which means that, as previously seen, the particle mass is significantly lower with HVO.

3.3 Soot oxidation reactivity

Figure 6 (top) shows the normalized differential mass conversion (Gram–Schmidt) of the tested soot samples of the different air–fuel-ratios and the different fuels. Furthermore, the temperatures T_{Max} calculated from the TGA profiles at the maximum conversion rate are shown in Fig. 6 (bottom).

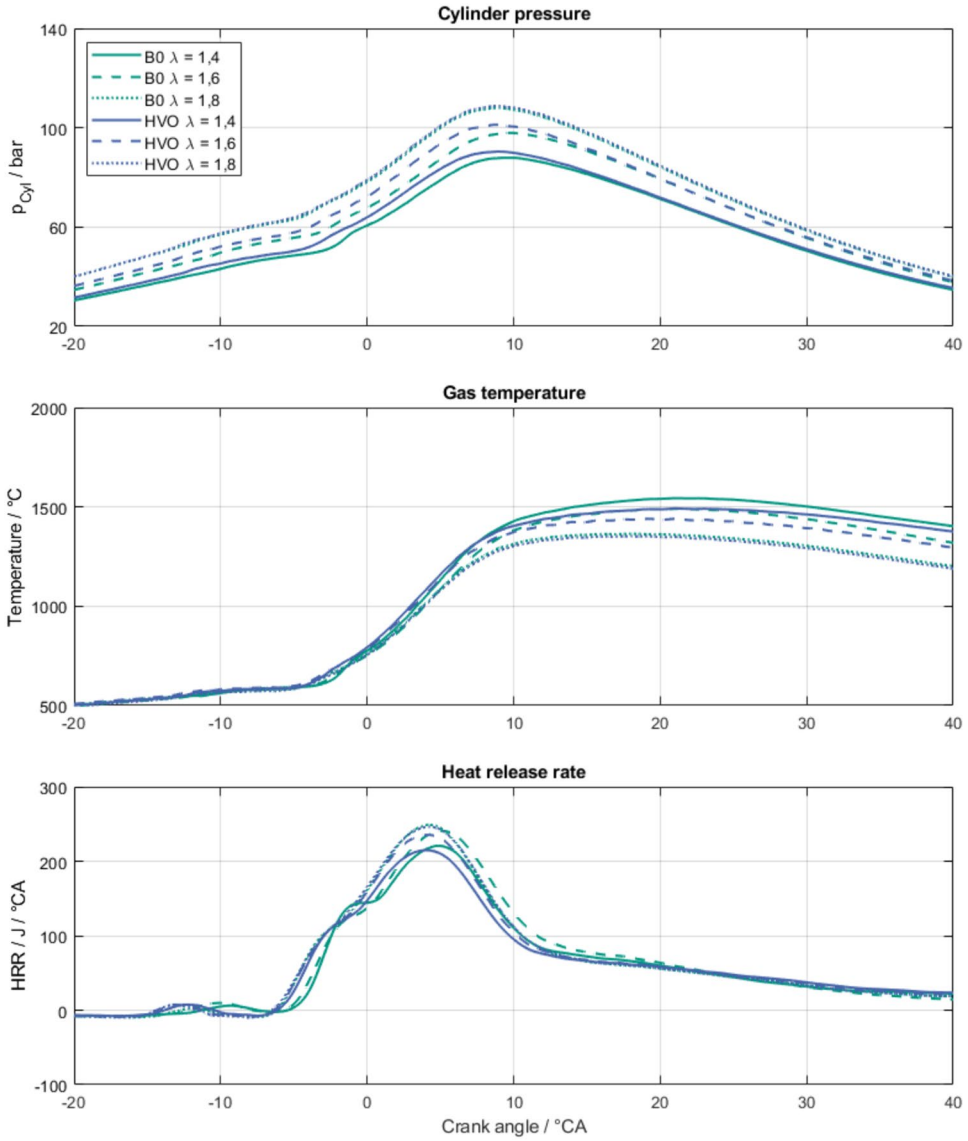

Fig. 3 Thermodynamic analysis of the air–fuel-ratio

The resulting soot reactivity indices RI according to (1) are also shown. As the air–fuel-ratio increases, the temperature at maximum conversion rate decreases, resulting in a corresponding increase in reactivity. This behavior can be explained by the decrease in the number of particles and the decrease in particle mass, which is consequently due to reduced soot formation [5, 6]. Accordingly, the lowest reactivity, which is reflected by the soot reactivity index, is at an air–fuel-ratio of $\lambda = 1.4$ and thus the highest T_{Max}. This trend is independent of the fuel used. Furthermore, it can be seen that a pronounced low-temperature peak occurs at an air–fuel-ratio of $\lambda = 1.8$ for both fuels, which indicates, for example, decomposing oxygen groups. However, it is particularly noticeable that the reactivity when operating with HVO is significantly lower than with fossil diesel, as HVO has significantly lower particle mass emissions in comparison. The increased number of particles of HVO with reduced particle mass favors the surface to volume ratio, whereby the reactivity should be significantly increased due to the better reaction of the oxygen molecules with the soot surface [8, 9, 25, 26]. Accordingly, it is assumed that the difference lies in the soot structure. Jansma et al. [15] attributed the difference to the lack of aromatics in the fuel, which ensure a more disordered soot structure. The smallest difference in terms of reactivity can be seen at an air–fuel-ratio of $\lambda = 1.4$. However, as can be seen in Fig. 3, the higher proportion of premixed combustion when using fossil diesel may be the decisive factor here.

4 Conclusion

The aim of this work was to investigate the soot oxidation reactivity of different air–fuel-ratios and to compare fossil diesel and HVO. The soot reactivity was determined by

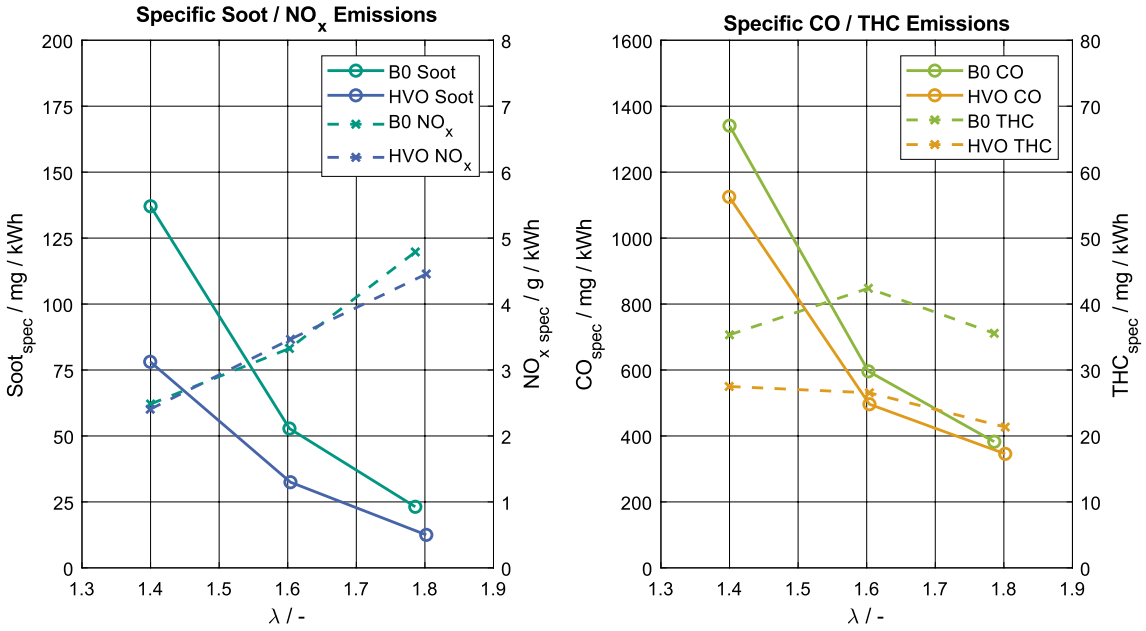

Fig. 4 Specific soot, NO_x, CO and THC emissions

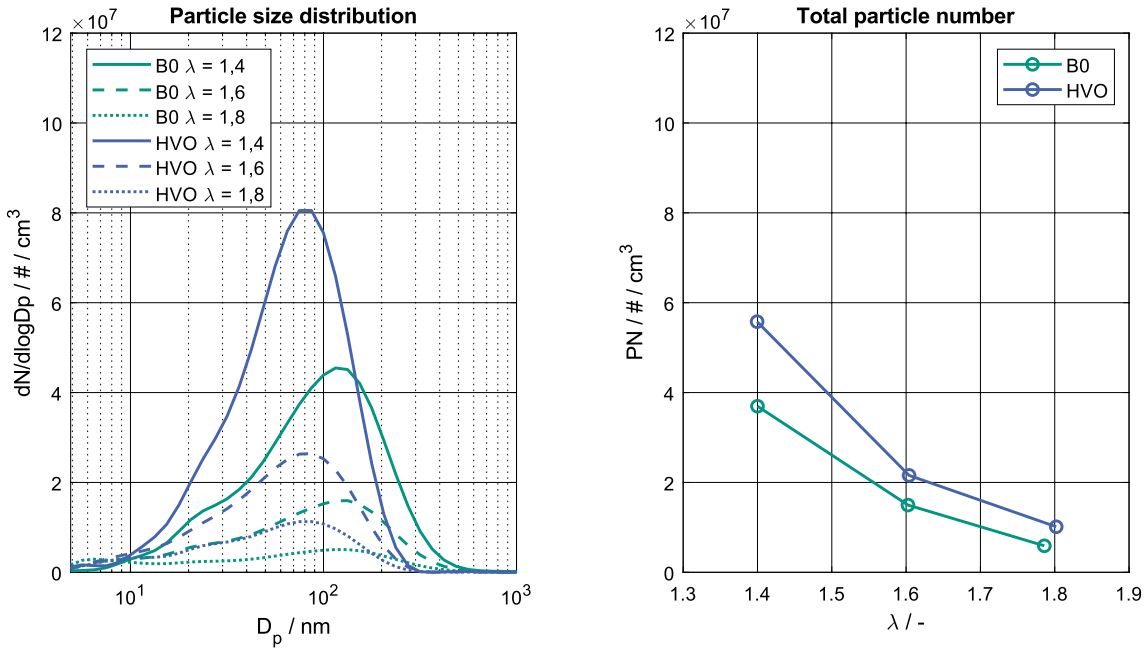

Fig. 5 Particle size distribution and total particle number

means of thermogravimetric analysis. The thermodynamic influences, gaseous emissions and particulate emissions were also examined. It was shown that the thermodynamic processes hardly differ, only the start of combustion is slightly earlier in the tests with HVO than with fossil diesel. This is due to the shorter ignition delay time due to the higher cetane number of HVO. It should also be noted that the soot mass, CO and THC emissions when operating with HVO are significantly lower than the emissions when operating with fossil diesel, regardless of the air–fuel ratio. NO_x emissions are at almost the same level when running on HVO. A disadvantage, however, is the increased number of particles when operating with HVO. Due to the shift to a smaller average particle size diameter,

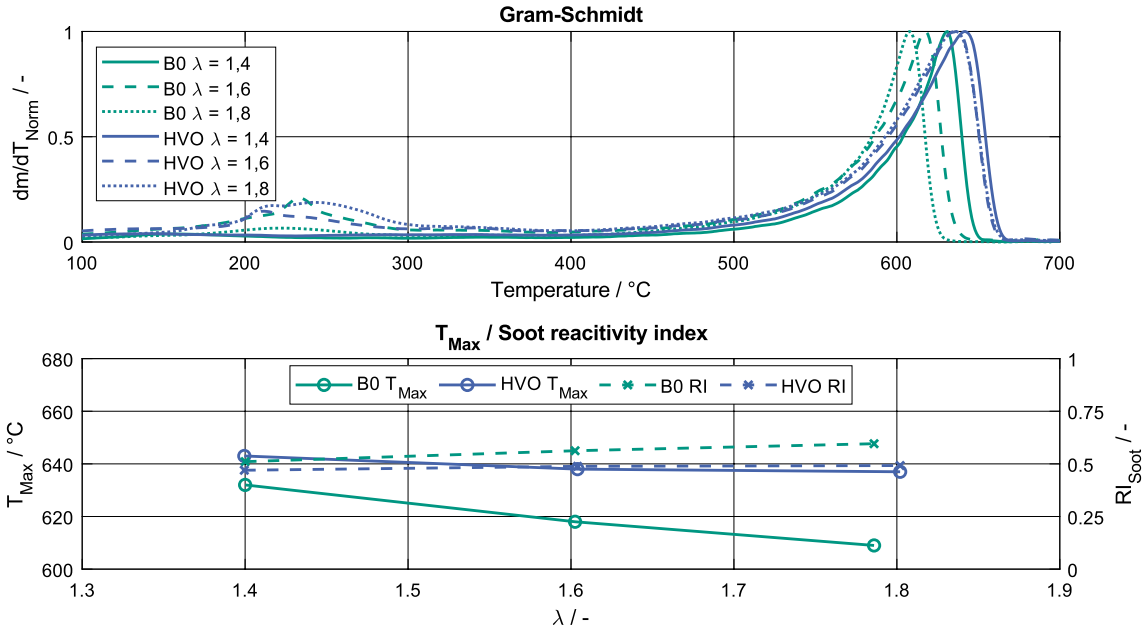

Fig. 6 Gram–Schmidt diagram, maximum oxidation temperature and soot reactivity index

there is nevertheless a reduction in soot mass compared to fossil diesel, as described above. With regard to soot reactivity, it was shown that reactivity increases with increasing air–fuel-ratio due to the decrease in particle mass and particle number. In addition to the engine parameters, the influence of the fuel also showed remarkable differences. The use of HVO showed a significant reduction in reactivity, although increased reactivity was to be expected both in terms of emissions and thermodynamically when operating with HVO. It is hypothesized that the reduced reactivity when operating with HVO is related to the modified structure of the soot due to the lack of aromatics. To evaluate this in relation to DPF regeneration, it is important to note that despite the potentially higher temperatures required for regeneration when running on HVO compared to fossil diesel, or may lead to slightly longer regeneration times, the reduction in soot emissions more than compensates for the lower reactivity. Especially at lower air–fuel-ratios, the ΔT_{Max} values are only around 10 °C apart. In future research, the soot samples will be investigated using high-resolution transmission electron microscopy, which enables a precise analysis of the soot structure. Furthermore, individual aromatics will be added to the fuel in order to investigate whether and which aromatics have an influence on the soot.

Acknowledgements The work was done within the KIT Helmholtz-Program MTET: Materials and Technologies for the Energy Transition Subtopic Technical Fuel Assessment and the support is gratefully acknowledged.

Author contributions C.B. wrote the main text of the manuscript and created the figures. All authors reviewed the manuscript.

Funding Open Access funding enabled and organized by Projekt DEAL.

Data availability No datasets were generated or analyzed during the current study.

Declarations

Conflict of interest The authors declare that there are no competing interests.

References

1. Lindner, S., Massner, A., Gärtner, U., et al.: Rußreaktivität bei Nutzfahrzeug-Dieselmotoren. MTZ Motortech Z **75**, 74–79 (2014). https://doi.org/10.1007/s35146-014-0324-6
2. Mehring, M., Elsener, M., Kröcher, O.: Development of a TG-FTIR system for investigations with condensable and corrosive gases. J. Therm. Anal. Calorim.Calorim. **105**, 545–552 (2011). https://doi.org/10.1007/s10973-010-1178-x
3. Huang, Y., Ng, E.C., Surawski, N.C., et al.: Effect of diesel particulate filter regeneration on fuel consumption and emissions performance under real-driving conditions. Fuel **320**, 123937 (2022). https://doi.org/10.1016/j.fuel.2022.123937
4. Vander Wal, R.L., Tomasek, A.J.: Soot oxidation. Combust. Flame **134**, 1–9 (2003). https://doi.org/10.1016/S0010-2180(03)00084-1
5. Lindner, S., Massner, A., Gärtner, U., et al.: Impact of engine combustion on the reactivity of diesel soot from commercial vehicle engines. Int. J. Engine Res. **16**, 104–111 (2015). https://doi.org/10.1177/1468087414563360
6. Schubiger, R.A., Boulouchous, K., Eberle, M.K.: Rußbildung und Oxidation bei der dieselmotorischen Verbrennung. MTZ Motortech Z **63**, 342–353 (2002). https://doi.org/10.1007/BF03227355
7. Rinkenburger, A., Toriyama, T., Yasuda, K., et al.: Catalytic Effect of potassium compounds in soot oxidation. ChemCatChem **9**, 3513–3525 (2017). https://doi.org/10.1002/cctc.201700338
8. Su, D.S., Müller, J.-O., Jentoft, R.E., et al.: Fullerene-like soot from euroiv diesel engine: consequences for catalytic automotive pollution control. Top. Catal.Catal. **30**(31), 241–245 (2004). https://doi.org/10.1023/B:TOCA.0000029756.50941.02
9. Chughtai, A.R., Kim, J.M., Smith, D.M.: The effect of air/fuel ratio on properties and reactivity of combustion soots. J. Atmos. Chem. **43**, 21–43 (2002). https://doi.org/10.1023/A:1016131112199
10. Mehring, M., Elsener, M., Kröcher, O.: Mikroanalytik und reaktivit ät von dieselpartikeln. MTZ. Motortech. Z. **72**, 690–697 (2011). https://doi.org/10.1365/s35146-011-0155-7
11. Song, J., Alam, M., BOEHMAN A, et al.: Examination of the oxidation behavior of biodiesel soot. Combust. Flame **146**, 589–604 (2006). https://doi.org/10.1016/j.combustflame.2006.06.010
12. Lapuerta, M., Oliva, F., Agudelo, J.R., et al.: Effect of fuel on the soot nanostructure and consequences on loading and regeneration of diesel particulate filters. Combust. Flame **159**, 844–853 (2012). https://doi.org/10.1016/j.combustflame.2011.09.003
13. Müller, J.-O., Su, D.S., Jentoft, R.E., et al.: Morphology-controlled reactivity of carbonaceous materials towards oxidation. Catal. Today. Today **102–103**, 259–265 (2005). https://doi.org/10.1016/j.cattod.2005.02.025
14. Sadezky, A., Muckenhuber, H., Grothe, H., et al.: Raman microspectroscopy of soot and related carbonaceous materials: spectral analysis and structural information. Carbon **43**, 1731–1742 (2005). https://doi.org/10.1016/j.carbon.2005.02.018
15. Jansma, H., Fino, D., Uitz, R., et al.: Influence of diesel fuel characteristics on soot oxidation properties. Ind. Eng. Chem. Res. **51**, 7559–7564 (2012). https://doi.org/10.1021/ie201823u
16. Tschöke, H., Marohn, R.: Tagung Einspritzung und Kraftstoffe2018. Springer Fachmedien Wiesbaden, Wiesbaden (2019). https://doi.org/10.1007/978-3-658-23181-1
17. Kitano, K., Sakata, I., Clark, R.: Effects of GTL fuel properties on DI diesel combustion. In: SAE Technical Paper Series. SAE International400 Commonwealth Drive, Warrendale (2005). https://doi.org/10.4271/2005-01-3763
18. Barbella, R., Ciajolo, A., D'Anna, A., et al.: Effect of fuel aromaticity on diesel emissions. Combust. Flame **77**, 267–277 (1989). https://doi.org/10.1016/0010-2180(89)90134-X
19. Erforth, D., Lagaly, P., Koch, T.: Interaction and influence of HVO-based fuels on diesel combustion. In: Liebl, J., Beidl, C., Maus, W. (eds.) Internationaler Motorenkongress, pp. 305–324. Springer Fachmedien Wiesbaden, Wiesbaden (2020). https://doi.org/10.1007/978-3-658-30500-0
20. Bogarra, M., Herreros, J.M., Tsolakis, A., et al.: Gasoline direct injection engine soot oxidation: fundamentals and determination of kinetic parameters. Combust. Flame **190**, 177–187 (2018). https://doi.org/10.1016/j.combustflame.2017.11.027
21. Hagen, F.P., Hardock, F., Koch, S., et al.: Why soot is not alike soot: a molecular/nanostructural approach to low temperature soot oxidation. Flow Turbul. Combust.Turbul. Combust. **106**, 295–329 (2021). https://doi.org/10.1007/s10494-020-00205-2
22. Lu, T., Cheung, C.S., Huang, Z.: Size-resolved volatility, morphology, nanostructure, and oxidation characteristics of diesel particulate. Energy Fuels **26**, 6168–6176 (2012). https://doi.org/10.1021/ef3010527
23. Niessner, R.: The many faces of soot: characterization of soot nanoparticles produced by engines. Angew. Chem. Int. Ed. Engl.. Chem. Int. Ed. Engl. **53**, 12366–12379 (2014). https://doi.org/10.1002/anie.201402812
24. Muller, P.: Glossary of terms used in physical organic chemistry (IUPAC Recommendations 1994). Pure Appl. Chem. **66**, 1077–1184 (1994). https://doi.org/10.1351/pac199466051077
25. Koch, S., Kubach, H., Velji, A., et al.: Impact of the injection strategy on soot reactivity and particle properties of a GDI Engine. In: SAE Technical Paper Series. SAE International400 Commonwealth Drive, Warrendale (2020). https://doi.org/10.4271/2020-01-0392
26. Koch, S., Hagen, F.P., Büttner, L., et al.: Influence of global operating parameters on the reactivity of soot particles from direct injection gasoline engines. Emiss Control Sci Technol **8**, 9–35 (2022). https://doi.org/10.1007/s40825-022-00211-y